Temporally and spatially partitioned neuropeptide release from individual clock neurons

Markus K. Klose[a], Marcel P. Bruchez[b,c,d], David L. Deitcher[e], and Edwin S. Levitan[a,1]

[a]Department of Pharmacology and Chemical Biology, University of Pittsburgh, Pittsburgh, PA 15261; [b]Molecular Biosensor and Imaging Center, Carnegie Mellon University, Pittsburgh, PA 15213; [c]Department of Chemistry, Carnegie Mellon University, Pittsburgh, PA 15213; [d]Department of Biological Sciences, Carnegie Mellon University, Pittsburgh, PA 15213; and [e]Department of Neurobiology and Behavior, Cornell University, Ithaca, NY 14853

Edited by Michael Rosbash, Howard Hughes Medical Institute, Waltham, MA, and approved March 21, 2021 (received for review January 29, 2021)

Neuropeptides control rhythmic behaviors, but the timing and location of their release within circuits is unknown. Here, imaging in the brain shows that synaptic neuropeptide release by *Drosophila* clock neurons is diurnal, peaking at times of day that were not anticipated by prior electrical and Ca^{2+} data. Furthermore, hours before peak synaptic neuropeptide release, neuropeptide release occurs at the soma, a neuronal compartment that has not been implicated in peptidergic transmission. The timing disparity between release at the soma and terminals results from independent and compartmentalized mechanisms for daily rhythmic release: consistent with conventional electrical activity–triggered synaptic transmission, terminals require Ca^{2+} influx, while somatic neuropeptide release is triggered by the biochemical signal IP_3. Upon disrupting the somatic mechanism, the rhythm of terminal release and locomotor activity period are unaffected, but the number of flies with rhythmic behavior and sleep–wake balance are reduced. These results support the conclusion that somatic neuropeptide release controls specific features of clock neuron–dependent behaviors. Thus, compartment-specific mechanisms within individual clock neurons produce temporally and spatially partitioned neuropeptide release to expand the peptidergic connectome underlying daily rhythmic behaviors.

fluorogen-activating protein | peptidergic transmission | synapse | neuropeptide release | circadian

Neuropeptides control development, synaptic function, and behaviors including feeding, pain perception, and sleeping. Studies of neuropeptide release within neural networks began with immunodetection of neuropeptide-content decreases (1, 2). However, this approach is only applicable when neuropeptide release is dramatic and relies on assuming that transport, capture, and degradation of neuropeptide-containing dense-core vesicles (DCVs) do not contribute to measured changes. Given that detecting neuropeptide release at living synapses is challenging, recent studies have measured somatic electrical activity and Ca^{2+} as surrogates for action potential–evoked Ca^{2+} influx that triggers synaptic release. Yet, the fidelity of these surrogates for peptidergic transmission has not been ascertained.

Indeed, these indirect approaches do not always provide a clear consensus about the timing of neuropeptide release. For example, in *Drosophila* small and large ventral lateral (s-LNv and l-LNv) clock neurons, which participate in circadian rhythms and the control of sleep, membrane excitability peaks slowly near sunrise, while cytosolic Ca^{2+} in l-LNv neurons slowly peaks near midday, ∼7 h after the s-LNv neurons (3–5). To resolve this discrepancy, we explored whether a recently developed optical approach that detects when and where neuropeptide release occurs at peripheral synapses based on a fluorogen-activating protein (FAP) (6) can be applied to central clock neurons. In contrast to neuropeptides tagged with fluorescent proteins, including variants sensitive to Ca^{2+} and H^+ (e.g., refs. 7, 8), FAPs produce no fluorescence until they bind their cognate nonfluorescent fluorogen. Thus, combining extracellular membrane–impermeant fluorogen with a DCV-targeted FAP currently provides the highest sensitivity for imaging neuropeptide release at native synapses.

Here, neuropeptide release by s-LNv and l-LNv clock neurons is resolved in the intact *Drosophila* brain. Synaptic release is found to be rhythmic but occurs with timing that was not evident from electrical or Ca^{2+} recordings. Even more remarkable, the soma, an unconsidered compartment for release in connectome and physiology studies, is a site of endogenous release that occurs with a different daily schedule than terminals. Genetically disabling the rhythmic somatic release trigger alters features of daily locomotor activity and sleep. Thus, distinct neuronal compartments are demonstrated to use different release mechanisms that in turn control different aspects of rhythmic behavior.

Results

Timing and Location of Neuropeptide Release by Clock Neurons. We began by considering whether the circadian function of s-LNv and l-LNv neurons is preserved after expressing fluorescent neuropeptide sensors. For *Drosophila* s-LNv neurons, an early attempt showed that a green fluorescent protein (GFP)-tagged mammalian neuropeptide did not recapitulate endogenous rhythmic changes in pigment-dispersing factor (PDF) in s-LNv neuron terminals and somas (9) because of genetic background effects (10). However, we found that rhythmic changes in the native neuropeptide are recapitulated when GFP-tagged *Drosophila* preproinsulin-like peptide 2 (Dilp2-GFP) (11) is expressed in s-LNv neurons (*SI Appendix*, Fig. S1 *A* and *B*). Furthermore, the known absence of rhythmic

Significance

It is believed that electrical activity simultaneously stimulates widespread release sites in single neurons to elicit neuropeptide-dependent behaviors. However, optically detecting neuropeptide release in the intact brain shows that clock neurons release neuropeptides from different sites at different times of the day. This is possible because one neuronal compartment, the soma, uses biochemical signaling instead of electrical activity to evoke release. Disrupting somatic release affects specific features of circadian locomotor activity and sleep. Thus, neuropeptide release is elicited by independent triggers from distinct parts of clock neurons to engage different regions of behavior-regulating circuitry. This strategy for expanding the connectome may be used for other neuropeptide-dependent behaviors, such as feeding and pain perception.

Author contributions: M.K.K. and E.S.L. designed research; M.K.K. performed research; M.P.B. and D.L.D. contributed new reagents/analytic tools; M.K.K. and E.S.L. analyzed data; and M.K.K. and E.S.L. wrote the paper.

The authors declare no competing interest.

This article is a PNAS Direct Submission.

[1]To whom correspondence may be addressed. Email: elevitan@pitt.edu.

This article contains supporting information online at https://www.pnas.org/lookup/suppl/doi:10.1073/pnas.2101818118/-/DCSupplemental.

Published April 19, 2021.

changes in PDF content of l-LNv neurons (9) was also evident with Dilp2-GFP (*SI Appendix*, Fig. S1*C*).

The preservation of normal function led us to use the neuropeptide release indicator Dilp2-FAP (6). This sensor takes advantage of the crystal-like concentrations of secreted peptides in DCVs and the mL5** FAP, which multimerizes to bind with ∼20 pM affinity and confer fluorescence on malachite green (MG)-based fluorogens (12). Specifically, fusion with proDilp2 to target the FAP to the DCV lumen (where it colocalizes with Dilp2-GFP) and applying membrane-impermeant fluorogens extracellularly ensures that fluorescence is produced after fusion pores are formed as part of kiss and run exocytosis, which mediates synaptic neuropeptide release (6, 13). Initial characterization showed that this fluorescence is sustained, reflecting that the FAP–MG complex apparently does not pass through the narrow fusion pore, which readily conducts molecules up to 4.5 kDa but not a 55 kDa protein (6). Therefore, we reasoned that excised intact fly brains with Dilp2-FAP expressed selectively in LNv neurons could be incubated with membrane-impermeant fluorogens (MG-BTau or MG-TCarb) (14, 15) to yield a signal for the integrated peptide release over the incubation period. In medulla l-LNv terminals examined late at night, ongoing release was evident and, as

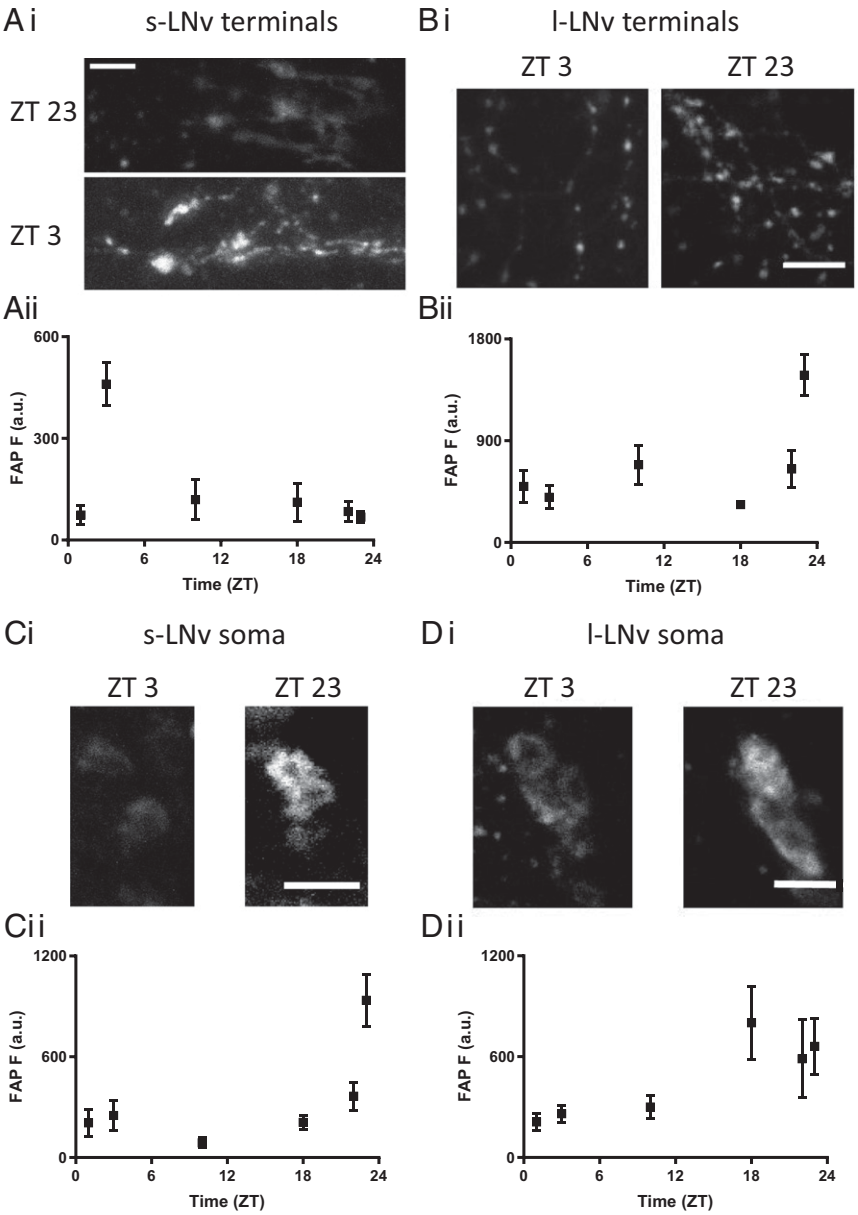

Fig. 1. Multicompartmental neuropeptide release by two subsets of ventrolateral clock neurons exhibits daily rhythms. (*Ai*) FAP images of neuropeptide release at s-LNv terminals in UAS-Dilp2-FAP/UAS-Dilp2-GFP; Pdf-Gal4 flies at ZT3 and ZT23 in entrained flies (12L:12D) (Scale bar, 10 μm). (*Aii*) Quantification of neuropeptide release from s-LNv terminals. n = for time points ZT 1, 3, 10, 18, 22, and 23 are 10, 22, 5, 7, 7, and 7, respectively. (*Bi*) Images of neuropeptide release at l-LNv nerve terminals at ZT3 and ZT23 (Scale bar, 10 μm). (*Bii*) Quantification of neuropeptide release by l-LNv nerve terminals across the day and night. n = for time points ZT 1, 3, 10, 18, 22, and 23 are 13, 9, 8, 7, 10, and 8, respectively. (*Ci*) Imaging shows release at s-LNv somas at ZT3 and ZT23 in entrained flies (12L:12D) (Scale bar, 10 μm). (*Cii*) Quantification of neuropeptide release by s-LNv somas across the day and night; note the large spike in release occurring at the end of the night (12L:12D). n= for time points ZT 1, 3, 10, 18, 22, and 23 are 18, 11, 10, 13, 17, and 14, respectively. (*Di*) Images of neuropeptide release in l-LNv somas during the morning (ZT3) and late night (ZT23) (Scale bar, 10 μm). (*Dii*) Neuropeptide release by l-LNv somas across the day and night. n = for time points ZT 1, 3, 10, 18, 22, and 23 are 12, 13, 6, 9, 9, and 10, respectively.

expected with conventional synaptic release, was enhanced with K^+-induced depolarization and inhibited by chelating extracellular Ca^{2+} with egtazic acid (EGTA) (*SI Appendix*, Fig. S2). Furthermore, circadian locomotor activity was preserved in animals expressing Dilp2-FAP in LNv neurons (*SI Appendix*, Table S1). With the feasibility of FAP-based endogenous release measurements established in the adult brain, this approach was used to measure neuropeptide release over 1 h periods at different times of the day in these rhythmically active neurons.

These experiments produced unexpected results. First, data from s-LNv and l-LNv terminals showed that the time of day for peak endogenous synaptic release do not correlate with the timing of electrical activity or Ca^{2+}: s-LNv neuron synaptic neuropeptide release peaks rapidly 3 h after sunrise (ZT3) (Fig. 1 *A*, *i* and *ii*) and is preceded by synaptic release by l-LNv neuron terminals, which occurs in a burst late at night (ZT23) (Fig. 1 *B*, *i* and *ii*). Although it remains possible that there are additional release peaks at time points that were not assayed experimentally, these data show that past activity and Ca^{2+} measurements were not sufficient for inferring the timing of neuropeptide release by clock neuron terminals.

Second, although neuronal somas have not been implicated previously in peptidergic transmission in vivo, FAP imaging revealed endogenous somatic neuropeptide release by LNv clock neurons (Fig. 1 *C* and *D*). Thus, previously reported rhythms in neuropeptide content (9) must reflect somatic release and possible yet to be discovered changes in transport and degradation.

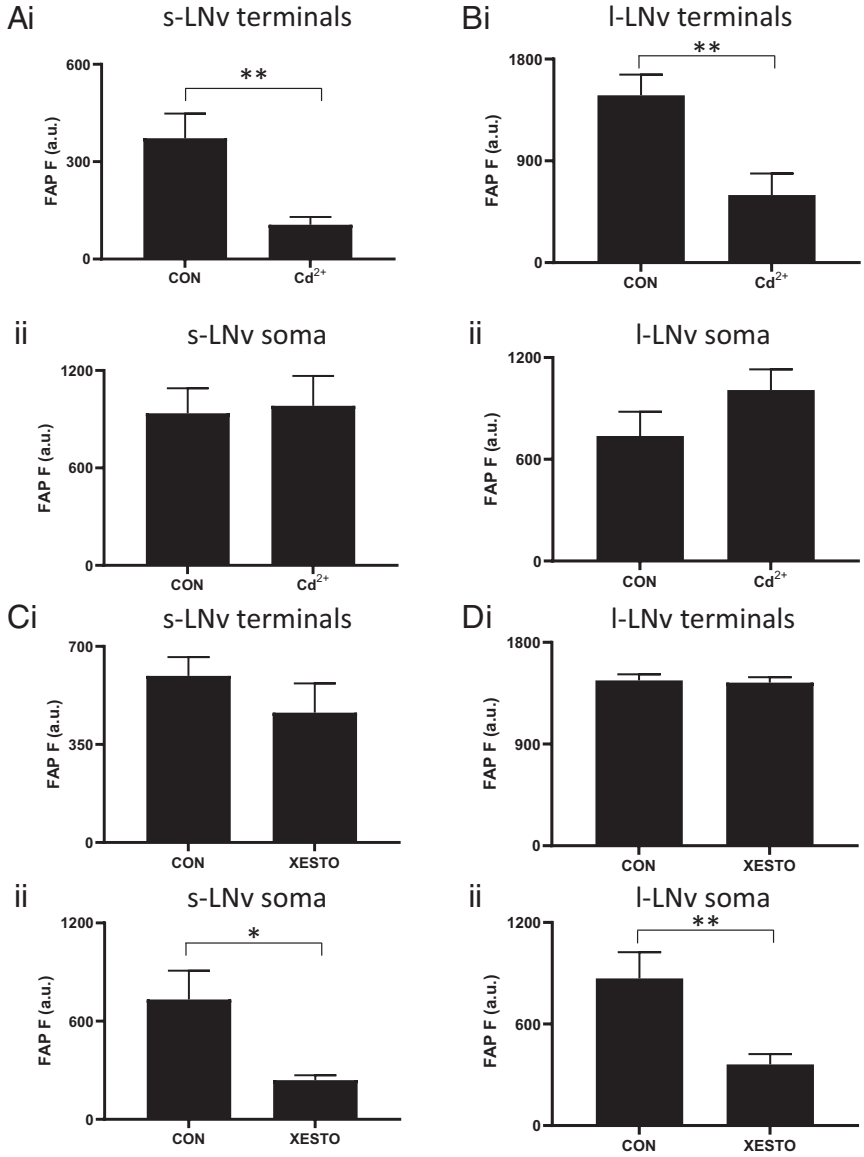

Fig. 2. Peak neuropeptide release requires Ca^{2+} influx into terminals and IP3 signaling in the soma. (*Ai*) Peak release (ZT3) by UAS-Dilp2-FAP; Pdf-Gal4 s-LNv terminals is inhibited by Cd^{2+} (10 μM, n = 13) compared to controls (n = 14). $^{**}P < 0.01$, unpaired *t* test. *ii* Peak release (ZT 23) by s-LNv somas is not affected by Cd^{2+} (10 μM, n = 13). For CON, n = 14). $P = 0.8493$, unpaired *t* test. (*Bi*) Peak release (ZT23) by l-LNv terminals is inhibited by Cd2+ (10 μM, n = 10) compared to controls (n = 8). $^{**}P < 0.01$, unpaired *t* test. *ii* Peak release (ZT 23) by l-LNv somas is not affected by Cd^{2+} (10 μM, n = 10). For CON, n = 8). $P = 0.8493$, unpaired *t* test. (*Ci*) Peak release (ZT3) by s-LNv terminals is not different between Xestospongin C (20 μM, n = 9) and control terminals (CON, n = 12). $P = 0.7951$, unpaired *t* test. *ii* Peak release (ZT23) by s-LNv somas is significantly reduced by Xestospongin C (20 μM, n = 19) compared to controls (CON, n = 24). $^{*}P < 0.05$, unpaired *t* test. (*Di*) Peak release (ZT23) by l-LNv terminals is not different between Xestospongin C (20 μM, n = 9) and controls (CON, n = 16). $P = 0.3126$, unpaired *t* test. *ii* Peak release (ZT 23) by l-LNv somas is reduced by Xestospongin C (20 μM, n = 16) compared to controls (CON, n = 21). $^{**}P < 0.01$, unpaired *t* test.

Even more remarkable, somatic release occurred hours earlier than release by distal terminals of the same neurons; peak somatic release by s-LNv neurons occurred at ZT23, while l-LNv neurons maintained an elevated release between ZT18 and ZT23 (Fig. 1 C and *D*, *ii*). Even though electrical signaling in this subset of neurons is required for normal clock circuit function and behavior (16), the different timing of release from terminals and the soma excludes propagating action potentials as the sole mechanism for evoking neuropeptide release.

Compartment-Specific Release Mechanisms. Because the effect of action potentials could be gated by other mechanisms, it was possible that electrical activity, which fluctuates slowly during the day, is necessary (but not sufficient) for release. This hypothesis predicts that inhibiting plasma membrane voltage-gated Ca^{2+} channels activated by action potentials should inhibit release throughout the neuron. Therefore, we examined the effect of the Ca^{2+} channel blocker Cd^{2+} on release by each compartment. Peak synaptic neuropeptide release was inhibited as expected, but somatic neuropeptide release was not affected in either s-LNv or l-LNv neurons (Fig. 2 *A* and *B*). These data imply that neuropeptide release by the soma, in contrast to release by terminals, does not require Ca^{2+} influx, thus excluding participation of action potentials in somatic release.

If electrical activity does not couple release from terminals and the soma, what mechanism is responsible for somatic neuropeptide release? Recently, FAP imaging demonstrated that there is spontaneous neuropeptide release, which is independent of extracellular Ca^{2+} and, in contrast to activity-dependent release, resistant to tetanus toxin (TetTx) (6). Therefore, sensitivity to TetTx is indicative of Ca^{2+}-dependent release. In fact, TetTx expression inhibited neuropeptide release by s-LNv and l-LNv somas (*SI Appendix*, Fig. S3 *A* and *B*). Release was also inhibited at s-LNv synapses (*SI Appendix*, Fig. S3*C*), but inhibition was not statistically significant at l-LNv synapses (*SI Appendix*, Fig. S3*D*). The latter result might be due to dilution of the TetTx upon cell-specific expression as l-LNv boutons are numerous and widely distributed. The failure to produce 100% inhibition at any of the release sites may explain why TetTx fails to disrupt circadian behaviors mediated by the neuropeptide PDF, which is an important clock signal released by s-LNv and l-LNv neurons (17, 18). More relevant here, significant TetTx inhibition suggests that somatic neuropeptide release is Ca^{2+} dependent.

The implication of Ca^{2+} dependence (*SI Appendix*, Fig. S3) without extracellular Ca^{2+} influx (Fig. 2 *A* and *B*) led us to examine the role of inositol trisphosphate (IP_3) receptors (IP3Rs), which mediate intracellular Ca^{2+} release from the endoplasmic reticulum into the cytosol. First, 100 nM Xestospongin C, a blocker of IP3Rs (19–21), was applied acutely. Strikingly, while peak endogenous neuropeptide release from terminals was unaffected, peak endogenous neuropeptide release from the soma was inhibited (Fig. 2 *C* and *D*). To independently test for a role for IP_3 signaling in somatic neuropeptide release, IP_3 sponge, which binds IP_3 to interfere with its second messenger function (21–23), was expressed along with the FAP reporter in LNv clock neurons and tested for effects on neuropeptide release at times of the day when release varies in terminals and the soma (ZT23 and ZT3, Fig. 1). Consistent with the Xestospongin C results, neuropeptide release from LNv terminals expressing IP_3 sponge remained rhythmic (Fig. 3 *A* and *B*, *i*), and peak somatic release at ZT23 was abolished (Fig. 3 *A* and *B*, *ii*), thus showing that the somatic release rhythm was disrupted. These data show that neuropeptide release by terminals does not depend on preceding somatic neuropeptide release. Furthermore, different neuronal compartments release neuropeptides at different times of the day by engaging different triggers (i.e., extracellular Ca^{2+} influx for terminals and IP_3 signaling for the soma).

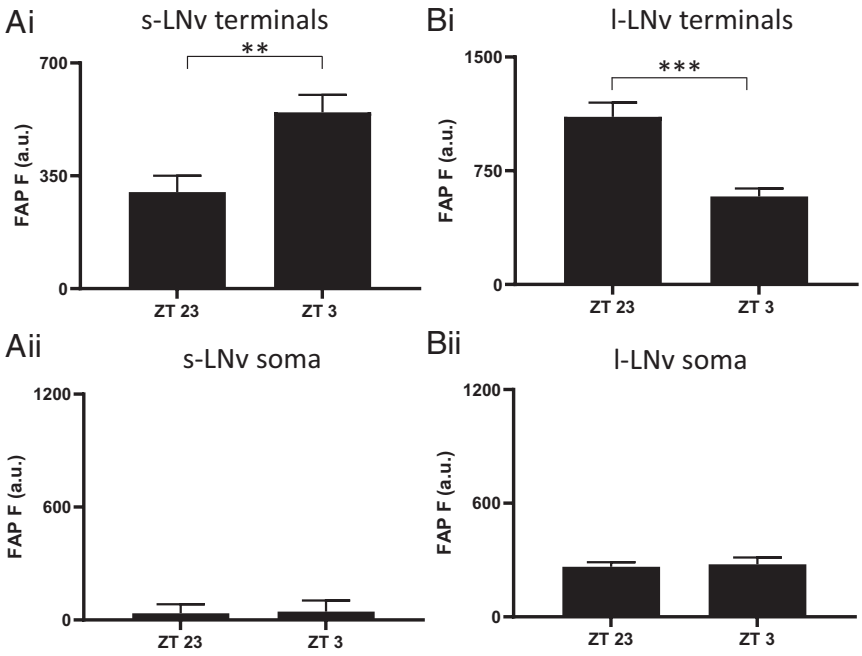

Fig. 3. IP3 sponge disrupts rhythmic somatic neuropeptide release in LNv clock neurons. (*Ai*) Circadian rhythms of neuropeptide release in s-LNv terminal of UAS-Dilp2-FAP; UAS-IP3 sponge/Pdf-Gal4 flies continued when IP3 signaling is disrupted through expression of IP3 sponge in PDF cells. Note the difference between ZT23 (n = 13) and ZT3 (n = 13), $^{**}P < 0.01$, unpaired *t* test. (*Aii*) Neuropeptide release from s-LNv somas is abolished when IP3 signaling is disrupted through expression of IP3 sponge in PDF cells. Note that there was no significant difference between ZT23 (n = 8) and ZT3 (n = 7), $P = 0.907$, unpaired *t* test. (*Bi*) Circadian rhythms in l-LNv terminal neuropeptide release continued when IP3 signaling is disrupted through expression of IP3 sponge in PDF cells. Note the difference between ZT23 (n = 6) and ZT3 (n = 6), $^{***}P < 0.001$, unpaired *t* test. (*Bii*) Neuropeptide release from l-LNv somas is interrupted when IP3 signaling is disrupted through expression of IP3 sponge in PDF cells. Note that there was no significant difference between ZT23 (n = 6) and ZT3 (n = 6), $P = 0.7690$, unpaired *t* test.

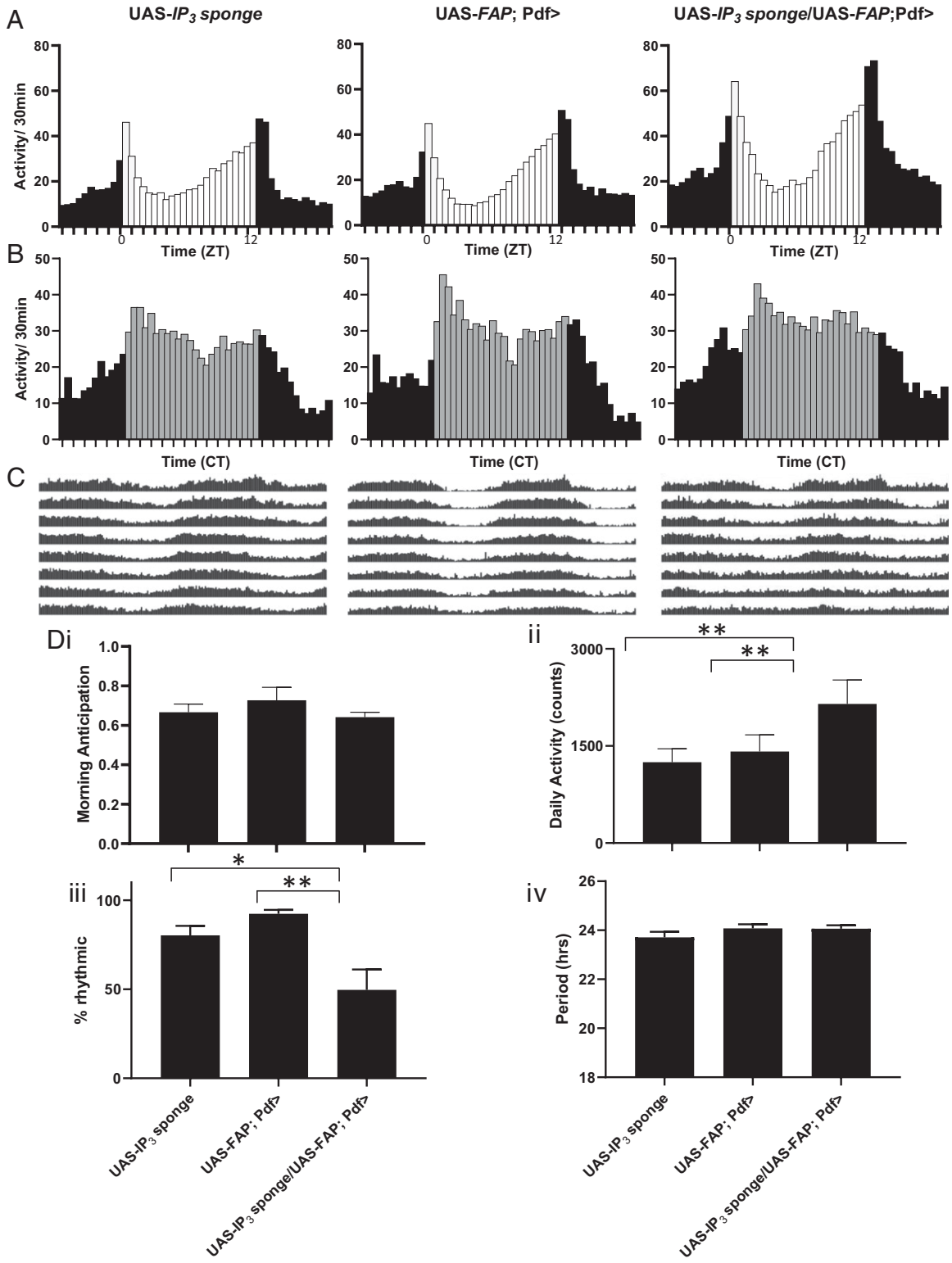

Fig. 4. IP3 signaling in LNv neurons suppresses locomotor activity and promotes rhythmicity. (*A*) LD (12 h: 12 h light:dark conditions) 5 to 7 group eductions for control UAS-IP3 sponge (n = 32), control UAS-FAP; Pdf-Gal4 (n = 32) and UAS-FAP; Pdf-Gal4/ UAS-IP3 sponge (n = 32) are shown. 12 h light (white bars):12 h dark (black bars). (*B*) DD1-2 group eductions. Constant darkness (gray bars indicate subjective day). (*C*) Average group actograms displayed in double plotted format over DD2-8. (*D*) Behavioral indices for each genotype including: *i* morning anticipation (repeated measures (RM) one-way ANOVA revealed no significant difference ($P = 0.1743$), *ii* total locomotor activity [RM one-way ANOVA revealed significant difference ($P < 0.01$)], *iii* Rhythmicity [RM one-way ANOVA revealed significant difference ($P < 0.01$)], and *iv* period [RM one-way ANOVA revealed no significant difference ($P = 0.3894$)]. *$P < 0.05$, **$P < 0.01$, Dunnett's multicomparison test.

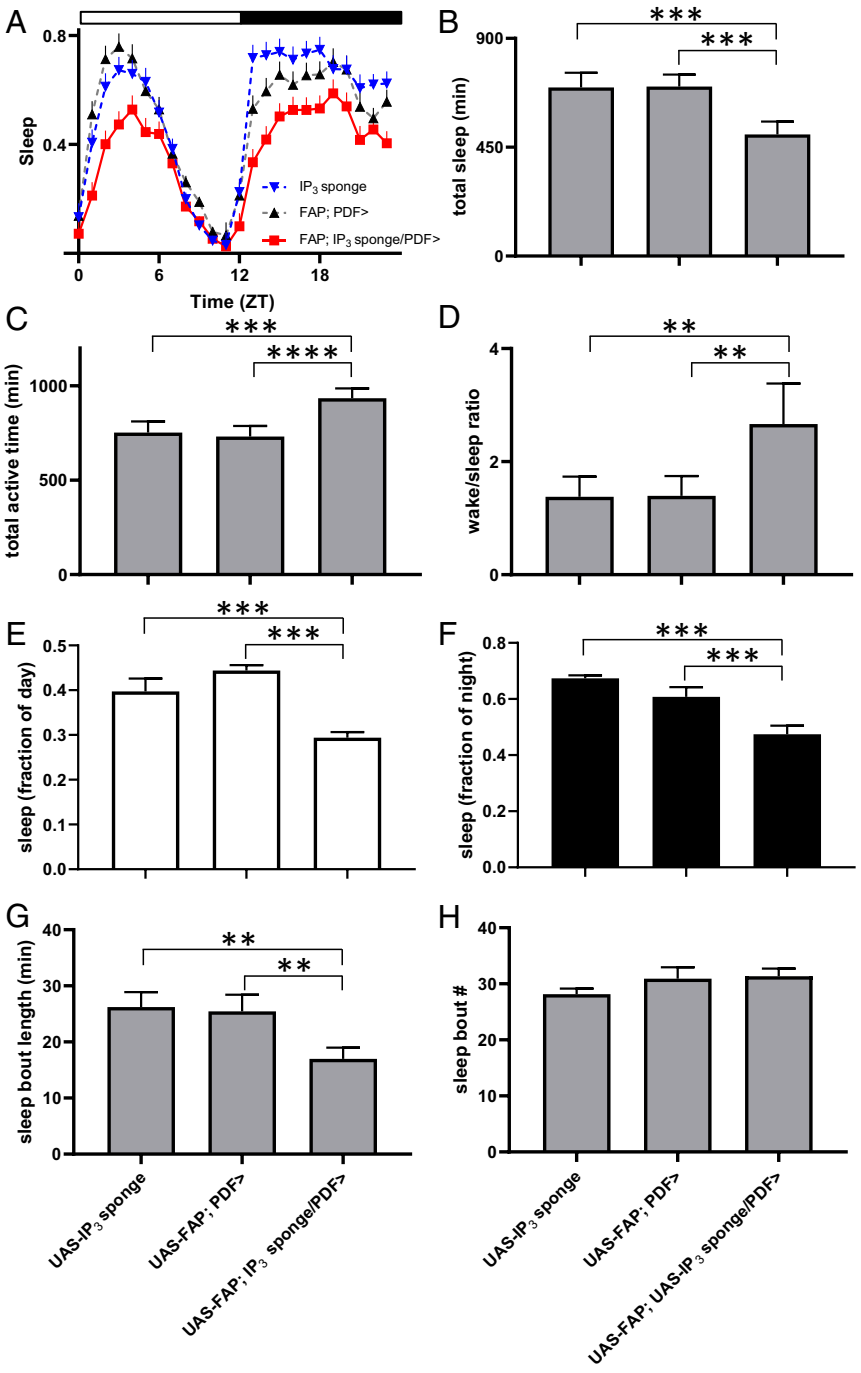

Fig. 5. IP3 signaling in LNv neurons increases total sleep time through promotion of sleep consolidation. (*A*) Sleep decreases in flies expressing IP3 sponge in PDF neurons (UAS-IP3 sponge/UAS-FAP; Pdf-Gal4) compared to two genetic controls (UAS-IP3 sponge and UAS-FAP; Pdf-Gal4). Sleep presented as fraction of each hour across the day. Flies entrained under a 12 h:12 h light/dark regimen. Data shown are from one experiment with 25 flies in each genotype. (*B*) Sponge expression in PDF neurons decreases total sleep by over 3 h compared to controls. A Repeated Measures (RM) one-way ANOVA revealed significant difference ($P < 0.001$). (*C*) Total active time. A RM one-way ANOVA revealed significant difference ($P < 0.001$). (*D*) Sleep/wake ratio. A RM one-way ANOVA revealed significant difference ($P < 0.001$). (*E*) Daytime sleep. A one-way ANOVA revealed significant difference ($P < 0.001$). (*F*) Nighttime sleep. A one-way ANOVA revealed significant difference ($P < 0.001$). (*G*) Sleep bout length. A RM one-way ANOVA revealed significant difference ($P < 0.01$). (*H*) Sleep bout number. A RM one-way ANOVA revealed no significant difference ($P = 0.1816$). Data analyzed from averages of five experiments. Total fly counts for each genotype: UAS-IP3 sponge/UAS-FAP; Pdf-Gal4 (n = 161), UAS-IP3 sponge (n = 164), and UAS-FAP; Pdf-Gal4 (n = 167). ****$P < 0.0001$, ***$P < 0.001$, **$P < 0.01$, Dunnett's multiple-comparison test.

Behavioral Effects of Compartmental Release Mechanisms. Transmission by the neuropeptide PDF from s-LNv neurons regulates several aspects of circadian behavior including morning anticipation, free-running rhythm period, and rhythmicity (24–27). Because IP_3 sponge selectively ablates somatic neuropeptide release, we examined the behavior of flies expressing IP_3 sponge in LNv neurons for effects on clock function behavioral output (Fig. 4 *A*–*C*). Expression of IP_3 sponge with Dilp2-FAP in LNv neurons did not affect morning anticipation or the period of daily locomotor rhythms but reduced the number of flies that

maintain rhythmic locomotor behavior compared to genetic controls and increased their daily activity (Fig. 4*D*).

The latter change (Fig. 4 *D*, *ii*) led us to consider whether sleep was affected. Quantification of sleep behavior revealed that the increase in overall activity was associated with reduced total sleep time and a large increase in the wake/sleep ratio (Fig. 5 *A*–*D*). Further analysis showed that the reduction in sleep was seen both during the day and the night (Fig. 5 *E* and *F*). Interestingly, average length of individual sleep bouts was shortened without a change in sleep bout number, thus revealing an effect on sleep consolidation (Fig. 5 *G* and *H*). Together with the circadian-locomotor–activity studies, these experiments identified numerous behavioral parameters (circadian period, morning anticipation, and sleep bout frequency) that remain normal when somatic release is inhibited. Thus, for those behaviors, synaptic neuropeptide release by terminals is sufficient. However, the experimental results also show that circadian rhythmicity and sleep consolidation rely on IP_3 in LNv neurons. The simplest interpretation of these experimental data is that the action potential independent somatic neuropeptide release influences a subset of parameters for clock neuron–dependent behaviors.

Discussion

FAP imaging revealed synaptic neuropeptide release from LNv clock neurons that does not conform to predictions from previously used indirect methods. Earlier neuropeptide-content measurements could not resolve whether somatic changes were due to release or traffic and did not detect l-LNv rhythmic neuropeptide release, likely because it is relatively modest and/or obscured by DCV capture that replenishes synaptic neuropeptide stores (11, 28). Furthermore, Ca^{2+} measured at the soma (5) was not reflective of release at terminals likely because of somatic IP_3 signaling. Thus, presynaptic Ca^{2+} may be more predictive of release by LNv termini. Finally, somatic electrical recording does not take into account regulation by presynaptic inputs. Thus, direct live imaging of neuropeptide release is essential for monitoring peptidergic transmission in the brain.

Indeed, this approach demonstrates that that central clock neurons release neuropeptide from terminals and the soma, with each compartment operating with different mechanisms and timing. Release from LNv clock neuron terminals is conventional (i.e., mediated by extracellular Ca^{2+} influx); because cell specific genetic Ca^{2+}-channel inhibition was not used, the contributions of Ca^{2+} channels in LNv neurons and their presynaptic inputs was not determined. In contrast, somatic neuropeptide release is triggered by IP_3 signaling that operates in the absence of action potential–induced Ca^{2+} influx. This shows that the two compartments use different mechanisms. It also raises the possibility that release by the two compartments differ in cell autonomy. Most importantly, different release mechanisms allow for multiphasic temporal control of neuropeptide release from separate compartments of the same neuron, each of which releases onto different parts of the clock circuit, thereby providing separate output avenues to independently influence different parameters of behavior.

Materials and Methods

Flies. All flies were reared on cornmeal/agar supplemented with yeast. Male flies were collected on the day of eclosion and maintained on a 12 h light:12 h dark photoperiod for physiological experiments. Flies were maintained at 25 °C. Genotypes include the following: 1) UAS-*Dilp2-GFP*; *Pdf*-Gal4, 2) UAS-*Dilp2-FAP*; *Pdf*-Gal4, 3) UAS-*Dilp2-FAP*/UAS-*Dilp2-GFP*; *Pdf*-Gal4, 4) UAS-*Dilp2-FAP*; UAS-*IP_3 sponge*, *Pdf*-Gal4, 5) UAS-*Dilp2-FAP*; UAS-*IP_3 sponge*. UAS-*Dilp2-GFP*, UAS-*Dilp2-FAP* and UAS-*IP_3 sponge* were described previously (6, 11, 22). Expression of tetanus toxin light chain and a control mutant (29) were induced by crosses to UAS (upstream activating sequence) lines (Bloomington #28838 and 28840).

Imaging. Experiments were performed on adult brain explants, bathed in HL3 saline, which contained (in mM) 70 mM NaCl, 5 KCl, 1.5 $CaCl_2$, 20 $MgCl_2$, 10 $NaHCO_3$, 5 trehalose, 115 sucrose, and 5 sodium Hepes, pH 7.2. Brains were dissected in Ca^{2+}-free HL3 saline (0.5 mM EGTA in place of Ca^{2+}), under red light to preclude activation of blue/green light-sensitive l-LNv neurons. Brains were transferred to HL3 saline and then placed in HL3-filled Sylgard chambers that were pretreated with poly-L-lysine, which acted as an adherent. To elicit depolarization-evoked release, HL3 was modified by increasing KCl to 70 mM by substituting NaCl.

Imaging data were acquired with an Olympus Fluoview 1000 upright confocal microscope with a 60× 1.0 numerical aperture water immersion objective. FAP signals were imaged with 640 nm excitation and Cy5 fluorescence optics, while GFP was imaged with a 473 nm excitation laser and standard fluorescein isothiocyanate optics. For FAP experiments, membrane-impermeant fluorogen (MG-B-Tau (Fig. 1) or MG-TCarb (Figs. 2–5) was added to the bathing solution at a final concentration of 1 μM. Endogenous release measurements (Figs. 2–5) were acquired after 60 min of bathing in the fluorogens in complete darkness. Two brains were placed in each dish of the same or differing genotypes

Quantification of fluorescence intensity was performed with ImageJ software (https:// imagej.nih.gov/ij/). For s-LNv–terminal GFP content, a region of interest (ROI) was drawn around the s-LNv dorsal protocerebral projection stack. l-LNv GFP terminal content was the average of 10 boutons for each hemisegment. For s-LNv and l-LNv terminal release, 6 to 10 boutons were averaged for each measurement. s-LNv and l-LNv soma measurements are the average of 2 to 4 ROIs from each hemisegment. Measurements from individual planes were made from each stack, and only the brightest measurement for each neuron was used in the average. Images were taken at several time points during both the day and night, and all measurements were background subtracted.

Behavior. Adult flies (3 to 4 d old) were loaded into glass tubes and placed in DAM2 Trikinetics Activity Monitors and entrained for 7 d on 12 h:12 h light:dark (LD) schedule, then released into constant darkness for 8 d. We assessed rhythmicity by normalizing activity from DD (12 h: 12 h dark:dark) days 2 to 8. We defined arrhythmic flies by rhythmicity threshold [Qp.act/Qp.sig] below 1 or a period estimate <18 or >30 h. Rhythmicity and period were assessed using ShinyR software (30).

Analysis. Statistical analysis and graphing were performed with Graphpad Prism software. Error bars represent SEM. Statistical comparison for two experimental groups was based on Student's *t* test. For multiple comparisons, one-way ANOVA was followed with Dunnett's posttest.

Chemicals. MG-B-tau and MG-TCarb were synthesized as previously described (14, 15). Pharmacological agents were bath applied in recording saline. Purchased chemicals included Xestospongin C (CAS Number: Abcam 88903-69-9) and cadmium chloride (SigmaAldrich).

Data Availability. Primary numerical data used to make figures have been deposited in Figshare (https://doi.org/10.6084/m9.figshare.14292257).

ACKNOWLEDGMENTS. We thank Dmytro Kolodieznyi (Carnegie Mellon University) for the preparation and characterization of the MG-TCarb dye, Michael Palladino (University of Pittsburgh) for use of his circadian activity monitoring incubator, and C. Andrew Frank (University of Iowa) for providing UAS-*IP_3 sponge* flies. This research was supported by NIH grants R01NS32385 and R21NS115023 to E.S.L. and RF1MH114103 and R21MH100612 to M.P.B.

1. P. H. Taghert, M. N. Nitabach, Peptide neuromodulation in invertebrate model systems. *Neuron* **76**, 82–97 (2012).
2. M. P. Nusbaum, D. M. Blitz, E. Marder, Functional consequences of neuropeptide and small-molecule co-transmission. *Nat. Rev. Neurosci.* **18**, 389–403 (2017).
3. G. Cao, M. N. Nitabach, Circadian control of membrane excitability in Drosophila melanogaster lateral ventral clock neurons. *J. Neurosci.* **28**, 6493–6501 (2008).
4. V. Sheeba, H. Gu, V. K. Sharma, D. K. O'Dowd, T. C. Holmes, Circadian- and light-dependent regulation of resting membrane potential and spontaneous action potential firing of Drosophila circadian pacemaker neurons. *J. Neurophysiol.* **99**, 976–988 (2008).
5. X. Liang, T. E. Holy, P. H. Taghert, Synchronous Drosophila circadian pacemakers display nonsynchronous Ca^{2+} rhythms in vivo. *Science* **351**, 976–981 (2016).
6. D. Bulgari *et al.*, Activity-evoked and spontaneous opening of synaptic fusion pores. *Proc. Natl. Acad. Sci. U.S.A.* **116**, 17039–17044 (2019).
7. N. V. Burke *et al.*, Neuronal peptide release is limited by secretory granule mobility. *Neuron* **19**, 1095–1102 (1997).

8. K. Ding *et al*., Imaging neuropeptide release at synapses with a genetically engineered reporter. *eLife* **8**, e46421 (2019).
9. J. H. Park *et al*., Differential regulation of circadian pacemaker output by separate clock genes in Drosophila. *Proc. Natl. Acad. Sci. U.S.A.* **97**, 3608–3613 (2000).
10. E. Kula, E. S. Levitan, E. Pyza, M. Rosbash, PDF cycling in the dorsal protocerebrum of the Drosophila brain is not necessary for circadian clock function. *J. Biol. Rhythms* **21**, 104–117 (2006).
11. M. Y. Wong *et al*., Neuropeptide delivery to synapses by long-range vesicle circulation and sporadic capture. *Cell* **148**, 1029–1038 (2012).
12. C. Szent-Gyorgyi *et al*., Malachite green mediates homodimerization of antibody VL domains to form a fluorescent ternary complex with singular symmetric interfaces. *J. Mol. Biol.* **425**, 4595–4613 (2013).
13. M. Y. Wong, S. L. Cavolo, E. S. Levitan, Synaptic neuropeptide release by dynamin-dependent partial release from circulating vesicles. *Mol. Biol. Cell* **26**, 2466–2474 (2015).
14. Q. Yan *et al*., Near-instant surface-selective fluorogenic protein quantification using sulfonated triarylmethane dyes and fluorogen activating proteins. *Org. Biomol. Chem.* **13**, 2078–2086 (2015).
15. C. P. Pratt *et al*., Tagging of endogenous BK channels with a fluorogen-activating peptide reveals β4-mediated control of channel clustering in cerebellum. *Front. Cell. Neurosci.* **11**, 337 (2017).
16. M. N. Nitabach, J. Blau, T. C. Holmes, Electrical silencing of Drosophila pacemaker neurons stops the free-running circadian clock. *Cell* **109**, 485–495 (2002).
17. E. Blanchardon *et al*., Defining the role of Drosophila lateral neurons in the control of circadian rhythms in motor activity and eclosion by targeted genetic ablation and PERIOD protein overexpression. *Eur. J. Neurosci.* **13**, 871–888 (2001).
18. M. Kaneko, J. H. Park, Y. Cheng, P. E. Hardin, J. C. Hall, Disruption of synaptic transmission or clock-gene-product oscillations in circadian pacemaker cells of Drosophila cause abnormal behavioral rhythms. *J. Neurobiol.* **43**, 207–233 (2000).
19. J. Gafni *et al*., Xestospongins: Potent membrane permeable blockers of the inositol 1,4,5-trisphosphate receptor. *Neuron* **19**, 723–733 (1997).
20. M. K. Klose, J. S. Dason, H. L. Atwood, G. L. Boulianne, A. J. Mercier, Peptide-induced modulation of synaptic transmission and escape response in Drosophila requires two G-protein-coupled receptors. *J. Neurosci.* **30**, 14724–14734 (2010).
21. T. D. James, D. J. Zwiefelhofer, C. A. Frank, Maintenance of homeostatic plasticity at the *Drosophila* neuromuscular synapse requires continuous IP_3-directed signaling. *eLife* **8**, e39643 (2019).
22. T. Uchiyama, F. Yoshikawa, A. Hishida, T. Furuichi, K. Mikoshiba, A novel recombinant hyperaffinity inositol 1,4,5-trisphosphate (IP(3)) absorbent traps IP(3), resulting in specific inhibition of IP(3)-mediated calcium signaling. *J. Biol. Chem.* **277**, 8106–8113 (2002).
23. K. Usui-Aoki *et al*., Targeted expression of Ip3 sponge and Ip3 dsRNA impaires sugar taste sensation in Drosophila. *J. Neurogenet.* **19**, 123–141 (2005).
24. S. C. Renn, J. H. Park, M. Rosbash, J. C. Hall, P. H. Taghert, A pdf neuropeptide gene mutation and ablation of PDF neurons each cause severe abnormalities of behavioral circadian rhythms in Drosophila. *Cell* **99**, 791–802 (1999).
25. S. Hyun *et al*., Drosophila GPCR Han is a receptor for the circadian clock neuropeptide PDF. *Neuron* **48**, 267–278 (2005).
26. C. Choi *et al*., Autoreceptor control of peptide/neurotransmitter corelease from PDF neurons determines allocation of circadian activity in drosophila. *Cell Rep.* **2**, 332–344 (2012).
27. M. Klose *et al*., Functional PDF Signaling in the Drosophila circadian neural circuit is gated by Ral A-dependent modulation. *Neuron* **90**, 781–794 (2016).
28. D. Shakiryanova, A. Tully, E. S. Levitan, Activity-dependent synaptic capture of transiting peptidergic vesicles. *Nat. Neurosci.* **9**, 896–900 (2006).
29. S. T. Sweeney, K. Broadie, J. Keane, H. Niemann, C. J. O'Kane, Targeted expression of tetanus toxin light chain in Drosophila specifically eliminates synaptic transmission and causes behavioral defects. *Neuron* **14**, 341–351 (1995).
30. K. Cichewicz, J. Hirsh, R.-D. A. M. Shiny, ShinyR-DAM: A program analyzing Drosophila activity, sleep and circadian rhythms. *Commun. Biol.* **1**, 25 (2018).